Available online at www.sciencedirect.com

ScienceDirect

Ceramics International 40 (2014) 4745–4751

CERAMICS INTERNATIONAL

www.elsevier.com/locate/ceramint

Diameter selective behavior of human nasal epithelial cell on Ag-coated TiO_2 nanotubes

Ming-Ying Lan[a,b], Sheng-Long Lee[c], Her-Hsiung Huang[d], Po-Fan Chen[e], Chia-Pei Liu[c], Sheng-Wei Lee[c,*]

[a]Department of Otolaryngology, Taipei Veterans General Hospital, Taipei City 11217, Taiwan, ROC
[b]Institute of Clinical Medicine, National Yang-Ming University, Taipei City 11221, Taiwan, ROC
[c]Institute of Materials Science and Engineering, National Central University, No. 300, Jhongda Road, Jhongli City 32001, Taiwan, ROC
[d]Department of Dentistry, National Yang-Ming University, Taipei City 11221, Taiwan, ROC
[e]Department of Chemistry, Tamkang University, New Taipei City 25137, Taiwan, ROC

Received 24 August 2013; accepted 5 September 2013
Available online 13 September 2013

Abstract

Titanium oxide (TiO_2), a light, strong, corrosion resistant, biocompatible and non-toxic metal, is widely used as dental or orthopedic implants, but is rarely used in nasal applications. There are three potential clinical applications for titanium in nasal surgery, including nasal septal perforation repairment, nasal reconstruction or rhinoplasty, and cerebral spinal fluid (CSF) rhinorrhea repairment. Nasal cavity is a contaminated cavity, thus to develop a nasal implant with antibacterial activity has its importance. We have developed self-organized TiO_2 nanotubes with different diameters by utilizing an electrochemical anodization method and further decorated the TiO_2 nanotubes with silver (Ag) layer by electron-beam deposition. The human nasal epithelial cells (HNEpCs) was used for evaluating the cytocompatibility of TiO_2 nanotubes with or without Ag decoration, including cell adhesion, cell proliferation assay for analyzing cell growth condition, and scanning electronic microscopy (SEM) for observing cell morphology. Furthermore, *Pseudomonus aeruginosa* was used for assessing the antibacterial activity of titanium implants. Our results showed that 25-nm-diameter Ag-coated TiO_2 nanotubes possess both good cytocompatibility with cultured HNEpCs and antibacterial activity against *P. aeruginosa*, as compared to 100-nm-diameter nanotubes. In conclusion, the small-diameter Ag-decorated TiO_2 nanotubes have high biocompatibility and good antibacterial activity, and there is potential of its usage for future clinical applications as novel nasal implants.

Keywords: Biocompatibility; TiO_2 nanotubes; Antibacterial; Human nasal epithelial cells; *Pseudomonas aeruginosa*

1. Introduction

Titanium (Ti) possesses several characteristics including high biocompatibility, corrosion resistance, being light weight and has been widely used as dental implants or bony implants. It forms a titanium oxide (TiO_2) layer on its surface (approximately 10 nm thick) which acts like a ceramic with excellent biocompatibility when it is exposed to air [1,2]. The current application of Ti in nasal surgery is still rare. There are three potential clinical applications for Ti and its alloys to be used in nasal surgery: nasal septal perforation repairment, nasal reconstruction or rhinoplasty, and cerebral spinal fluid (CSF) rhinorrhea repair.

Nasal septal perforation, which can be caused by tumor, trauma, long-term topical drug use like cocaine or decongestant nasal sprays, inflammatory, and infectious disease, is still a challenging problem for otolaryngologists [3–6]. Various surgical techniques, including advancement flaps and inferior turbinate flap, have been developed to repair septal perforation limited to defects of less than 3 cm in diameter [7,8]. Using Ti mesh with open rhinoplasty approach as a novel method to repair large septal perforation has been described with good results [9,10]. However, there were still some patients whose Ti meshes were not mucosalized completely during the

*Corresponding author. Tel.: +886 3 422 7151x34905; fax: +886 3 280 50 34.
E-mail addresses: swlee@ncu.edu.tw, schon0911@gmail.com (S.-W. Lee).

0272-8842/$ - see front matter © 2013 Elsevier Ltd and Techna Group S.r.l. All rights reserved.
http://dx.doi.org/10.1016/j.ceramint.2013.09.018

follow-up period [9]. Another application for Ti in nasal surgery is nasal reconstruction and rhinoplasty [11–14]. Henry has used Ti as the nasal scaffolding in the total nasal reconstruction of eight patients with post-operative nasal defect due to nasal cavity cancer with excellent cosmetic results [11]. Rodríguez-Prieto also demonstrated good functional and esthetic results without any rejection or other complications in his patients who received nasal reconstruction with Ti [13]. However, just like all other types of alloplastic materials, there were still cases in which implant extrusion or infection with Ti nasal implants were noted [11,15]. The third clinical application for Ti in nasal surgery is CSF rhinorrhea repair. Esposito used Ti in his cases of CSF leak repair using the endonasal approach with good results [16]. The nasal cavity has some distinct tissue characteristics: thin nasal mucosa and a contaminated cavity. Since there are often bacteria in nasal cavities, Ti with an antibacterial activity may prevent implant infection related meningitis in patients with CSF rhinorrhea.

Several factors control the biocompatibility of an implant, such as implant size, shape, material composition and surface characteristics. Among them, the surface characteristic of an implant is the most important factor [1,2]. In this study, we modified the Ti implant surface by generating a nanotube structure with silver (Ag) decoration. The human nasal epithelial cells (HNEpCs) were used to evaluate its biocompatibility and *Pseudomonus aeruginosa*, one of the most common bacteria found in sinonasal biofilm formation, was tested for its antibacterial effect. The small-diameter Ag-coated TiO_2 nanotubes revealed good biocompatibility and antibacterial effect. This design has the potential in future clinical applications. It may overcome the possible complications of current Ti nasal implants, such as implant extrusion and implant infection.

2. Material and methods

2.1. Material preparation

Generation of self-assembled TiO_2 nanotubes in a highly regular arrangement was achieved by anodizing Ti foil in the F-containing electrolyte. Commercially pure Ti foils with purity 99.7% (diameter of 12 mm; thickness of 0.127 mm) were used for producing nanotube surface. Polished Ti foils were ultrasonically cleaned in acetone, distilled water followed by alcohol before anodization. All anodization experiments were performed in ethylene glycol electrolytes containing 0.5 wt% NH_4F with different potentials at 20 °C for 90 min. A two-electrode electrochemical cell with Ti anode and platinum (Pt) as counter electrode were used. Anodization voltage was kept constant at 10 V, 20 V, and 40 V, respectively. Subsequently, a 10-nm thick Ag layer was electron-beam-evaporated on the nanotube surfaces. During the Ag deposition, vacuum level and deposition rate were kept at 2×10^7 Torr and 0.1 nm/s, respectively. Both these Ti sheets were cleaned by deionized water and sterilized with low-intensity ultraviolet (UV) light irradiation (< 2 mW/cm^2) using fluorescent black-light bulbs for 8 h before the following biocompatibility tests. The surface morphologies of Ag-free and Ag-coated TiO_2 nanotubes were characterized *ex situ* using field-emission scanning electron microscopy (FE-SEM).

2.2. Human nasal epithelial cell culture

Human Nasal Epithelial Cell (HNEpC) (PromoCell Bioscience Alive, Heidelberg, Germany) were plated in T25 cell culture flasks (Falcon, BD Biosciences, San Jose, CA, USA) and cultured with Airway Epithelial Cell Growth Medium (PromoCell Bioscience Alive, Heidelberg, Germany) containing bovine pituitary extract (0.004 mL/mL), human epidermoid growth factor (0.5 ng/mL), insulin (5 μg/mL), transferrin (10 μg/mL), hydrocortisone (0.5 g/mL), epinephrine (0.5 μg/mL), triiodo-l-thronine (6.7 ng/mL), retinoic acid (0.1 ng/mL), and phenol red (0.62 ng/mL). Cultures were maintained at 37 °C in a humidified atmosphere of 5% CO_2. Cells were then seeded on Ti sheets placed on the bottom of 12-well culture plate (Falcon, BD Biosciences, San Jose, CA, USA) at a density of 1×10^4/cm^2 for 3 days for cell adhesion and proliferation assays.

2.3. Cell adhesion assay

After cell plating on the Ti sheets for 3 days, the adherent cells were fixed for 1 h in 4% paraformaldehyde (USB Corp., Cleveland, OH, USA) at room temperature. Cells underwent two washes in PBS and were permeabilized with 0.1% Triton X-100 (Sigma-Aldrich Corporation, St. Louis, MO, USA) in PBS for 15 min at 4 °C. Cells were then washed with PBS and incubated with rhodamine phalloidin (Life Technologies Corporation, Grand Island, NY, USA) for 15 min at room temperature for actin filament stain and diamidino-2-phenylindole (DAPI; Thermo Fisher Scientific Inc., Waltham, MA, USA) for 5 min for nuclei stain. Cells were then analyzed under a fluorescent microscope (AX80, Olympus). The specimens were further characterized by using field emission scanning electron microscopy (FE-SEM; FEI Quanta 200F, FEI, Hillsboro, OR, USA). Briefly, after 3 days of cell incubation, cells were fixed with 2.5% glutaraldehyde solution (Merck & Co., Inc., Whitehouse Station, NJ, USA) for 1 h at room temperature. Samples were rinsed in PBS solution, dehydrated in a sequential series with mixtures of ethanol and distilled water (40, 50, 60, 70, 80, 90, and 100%) and critical point dried with a Critical Point Dryer (CPD 030, Leica Microsystems, Wetzlar, Germany). A thin Pt film was coated on the samples before SEM observation.

2.4. Cell proliferation assay

Cell viability was determined using the WST-1 cell proliferation reagent kit (Roche, Penzberg, Germany), according to the manufacturer's instructions. On the 3rd day after seeding the cells at a density of 1×10^4 cells/cm^2 on the Ti sheets, cells were washed with PBS twice, and incubated with medium containing 10% WST-1 cell proliferation reagent in a humidified atmosphere of 5% CO_2 at 37 °C for 2 h. The solution was then retrieved from each well to a 96-well plate and optical

density (OD) was measured using a spectrophotometer (Tecan Group Ltd., Männedorf, Switzerland) at 450 nm.

2.5. Antibacterial test

The antimicrobial activity of the Ti/Ag surface was tested against *P. aeruginosa* (ATCC15442, Bioresource Collection and Research Center, Hsinchu, Taiwan). Tryptic soy broth and tryptic soy agar were used to grow the bacteria. Titanium sheets (both control and silver-coated ones) were exposed to 150 μL bacterial solution containing *P. aeruginosa* with a concentration of 1.6×10^{10} colony forming units (CFU)/mL for 4 h at 37 °C to allow bacteria to adhere to the TiO_2 surface. After dipping sheets into sterile PBS to remove the detached bacteria, the plates were subsequently fixed with 2.5% glutaraldehyde solution (Merck & Co., Inc., Whitehouse Station, NJ, USA) for 1 h at room temperature. Samples were rinsed in PBS solution, dehydrated in a sequential series with mixtures of ethanol and distilled water (40, 50, 60, 70, 80, 90, and 100%) and critical point dried with a Critical Point Dryer (CPD 030, Leica Microsystems, Wetzlar, Germany). A thin Pt film was coated on the samples and evaluated by SEM.

2.6. Statistical analysis

All experiments were carried out in triplicate and at least three independent experiments were performed. The test values were expressed as mean ± standard error (SE). Statistical

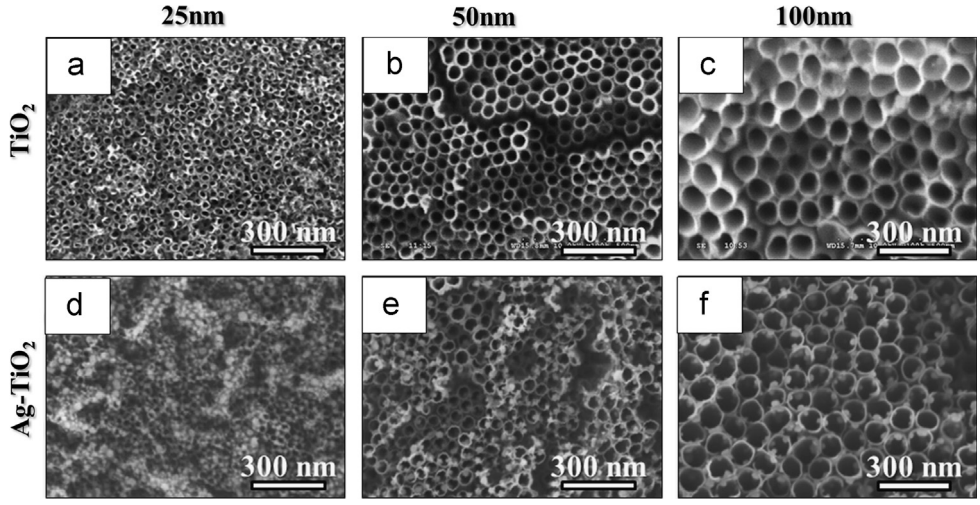

Fig. 1. SEM images of self-organized TiO_2 nanotubes with different diameters. The as-grown (a–c) and Ag-coated (d–f) nanotubes have the diameters of 25, 50, and 100 nm, respectively.

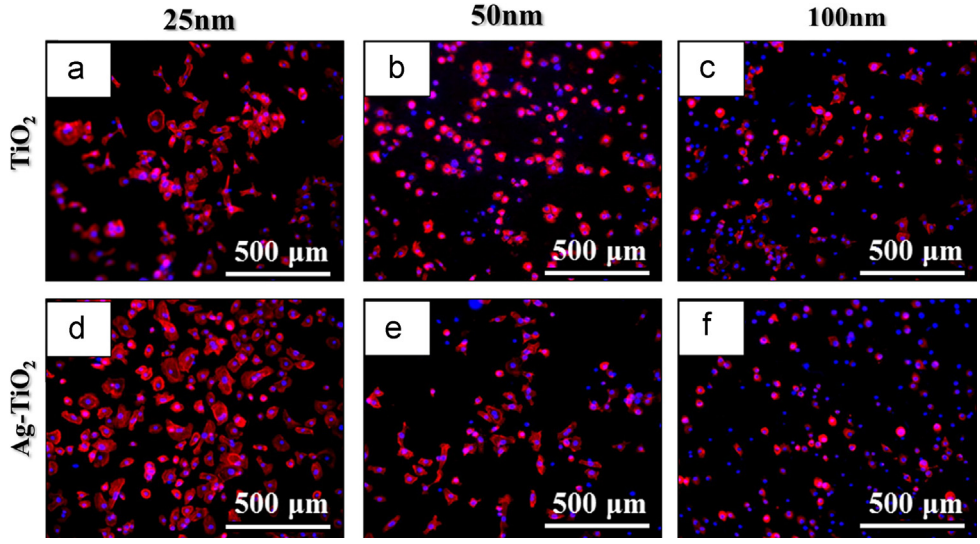

Fig. 2. Fluorescent images of the HNEpCs attachment on the as-grown (a–c) and Ag-coated (d–f) TiO_2 nanotubes of different diameters. The red fluorescence indicates cytoskeletal actin, and the blue fluorescence indicates cell nuclei. For both as-grown and Ag-decorated TiO_2 nanotubes, longer, better-defined actin cytoskeleton, and higher density of HNEpCs were noted on the smaller diameter nanotubes. (For interpretation of the references to color in this figure legend, the reader is referred to the web version of this article.)

comparisons of multigroup data were analyzed by ANOVA followed by the Sheffe posttest using SPSS 12.0 software (SPSS Inc.,Chicago, IL). A p value of < 0.05 was considered statistically significant.

3. Results

Fig. 1 shows the FE-SEM image of anodic TiO_2 nanotubes of different diameter size before (a–c) and after Ag deposition (d–f). The XRD results obtained from our previous study confirmed these TiO_2 nanotubes to be amorphous phase, mainly $TiO_2 \cdot xH_2O$ [17]. The size of the Ag particles decorated by e-gun vacuum evaporation system is between 10 nm and 15 nm, approximately. It can be seen that the Ag nanoparticles were homogeneous distributed on the top of the nanotube walls, except the 25-nm-diameter nanotubes, in which some local agglomeration on the surface was observed due to the limitation of the nanotube size.

To test the biocompatibility, cell adhesion test and cell viability test were performed. In cell adhesion assay, HNEpCs were used to culture on the surface of TiO_2 nanotubes with and without Ag decoration. Cytoskeleton actin which expressed red fluorescence was stained with rhodamine phalloidin, while cell nuclei expressed blue fluorescence was stained with DAPI. For both TiO_2 nanotubes with and without Ag deposition, better-defined actin cytoskeleton and higher density of HNEpCs were noted on the smaller-diameter TiO_2 nanotubes compared to those on the larger-diameter ones (Fig. 2). This may be due to the smaller-diameter TiO_2 nanotubes provide more focal points for cells to adhere then spread for further cell proliferation.

For detailed observation of cell adhesion, FE-SEM was further used to analyze the HNEpCs on different Ti sheets after a 3-days culturing. As shown in Fig. 3, the HNEpCs cultured on the 25-nm-diameter TiO_2 nanotubes reveal good cell adhesion with bigger cell morphology and better cytoskeleton development, while those on the 50-nm- and larger-diameter TiO_2 nanotubes show rounded and smaller cell morphology with lack of cell spreading. Lamellipodia and filopodia can even be observed on HNEpCs cultured on 25-nm-diameter Ag-coated TiO_2 nanotubes (see the insert of Fig. 3d).

WST-1 assay was further performed to quantitatively evaluate the condition of cell proliferation on the Ti sheets. Fig. 4 shows that both as-grown and Ag-coated 25-nm-diameter TiO_2 nanotubes have higher OD values than corresponding 50- and 100-nm-diameter ones in the cell proliferation test. In addition, the OD was lower on the Ag-coated TiO_2 nanotubes group compared to the same diameter as-grown group, although there was no statistically significant difference.

Fig. 5 demonstrated the results of the antibacterial test. The 25-nm-diameter as-grown TiO_2 nanotubes showed numerous *P. aeruginosa* adhered on it, while few *P. aeruginosa* were noted on same diameter Ag-coated ones (Fig. 5a and b). The result suggests that the Ag-coated TiO_2 nanotubes can efficiently inhibit the growth of the bacteria. Furthermore, some of the bacteria on the Ag-coated TiO_2 nanotubes presented with deformity as indicated by the arrows in Fig. 5d, which is not found in those on as-grown samples (Fig. 5c).

4. Discussion

Ti has several advantages when used in nasal implants for nasal reconstruction. It can resist the forces of contraction better than bone or cartilage, especially in patients who had undergone postoperative radiotherapy. It can provide adequate support to avoid the flutter phenomenon produced during inhalation; avoid harvesting natural cartilage or bone to reduce the risk of graft necrosis and prevent morbidity in the donor area; overcome possible problem of autologous materials insufficiency in cases of large nasal defects [13]. In addition,

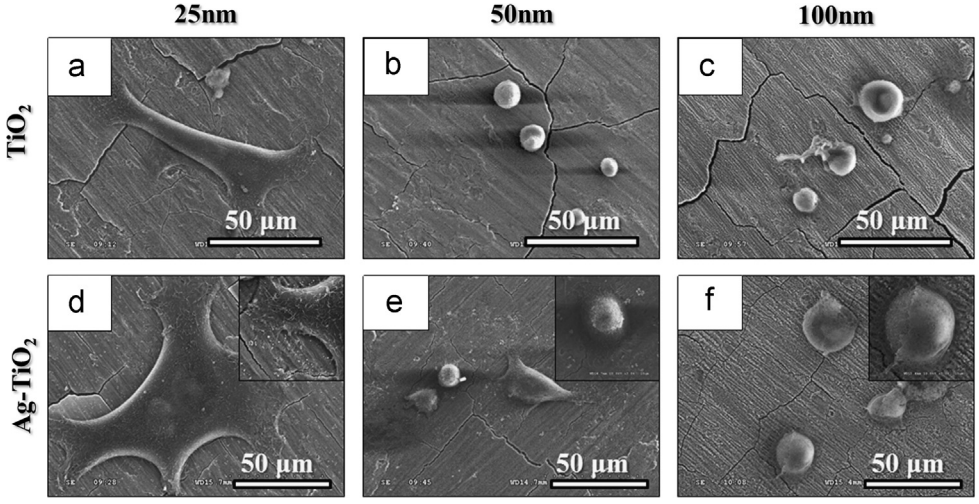

Fig. 3. SEM images showing the cell adhesion and proliferation of HNEpCs on the as-grown (a–c) and Ag-coated (d–f) TiO_2 nanotubes of different diameters. The HNEpCs cultured on the 25-nm-diameter nanotubes reveal good cell adhesion with an elongated cytoskeleton development, while those on the 50-nm-diameter or larger-diameter nanotubes show rounded cell morphology with lack of cell spreading in both as-grown and Ag-coated samples. Lamellipodia and filopodia can be observed on HNEpCs cultured on 25-nm- diameter Ag-coated TiO_2 nanotubes (the insert of (d)).

Ti can be molded into a desired shape, acting like a thin but strong supporting bridge which can be placed into the nose just through tiny incision in the nostril. In cases of CSF rhinorrhea repair, Ti also possesses several advantages: it provides relatively rigid support to hold the repair in position and prevent graft migration into either the sphenoid sinus or the intradural space by holding the graft against the edges of the bony and dural defect; it is malleable and easily configured to the bony defect; and it is easily visualized on CT and MRI scans, allowing its location to be easily confirmed [16]. Although there are many advantages with regards to Ti being used as nasal implants in nasal reconstruction and CSF rhinorrhea repair, implant extrusion is still a possible problem.

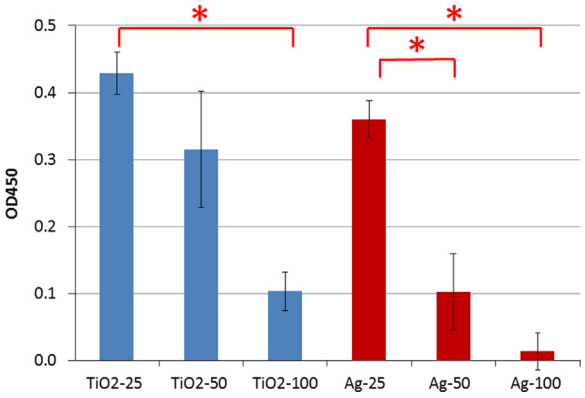

Fig. 4. Optical densities (OD) measured after the culture of HNEpCs on the as-grown and Ag-coated TiO_2 nanotubes of different diameters. Cell proliferation is lowest for the largest diameter of 100 nm in both as-grown and Ag-coated TiO_2 nanotubes. Meanwhile, the 25-nm-diameter as-grown sample shows the highest OD value of all nanotube samples. Data were means $\pm$ SE of three independent experiments ($^*p < 0.05$).

In order to reduce the implant extrusion rate, developing a more biocompatible Ti implant has its importance. In this study, we controlled the diameter of TiO_2 nanotubes by changing the anodization voltage. Three different tube sizes (25 nm, 50 nm, and 100 nm) were fabricated by 10 V, 20 V, and 40 V, respectively. One group of samples was further coated with Ag by electron-beam evaporation method. From the results, we can see that the smaller-diameter TiO_2 nanotubes with or without Ag decoration possess the best biocompatibility compared to larger-diameter ones. The HNEpCs on the 25-nm-diameter TiO_2 nanotubes reveal good cell adhesion with wide and flatten morphology, while those on the 50-nm- or larger-diameter nanotubes show more rounded morphology and lack of cell spreading. Besides, the smaller-diameter TiO_2 nanotubes showed the best cell proliferation. This may be due to that the predicted size of surface occupancy by the focal contact of a cell is about 10 nm in diameter, and a 15–25 nm spacing allows clustering of integrins with following optimal integrins activation, which finally results in better cell adhesion and then proliferation [18]. On the contrary, when the diameter of nanotubes is larger than 50 nm, the integrins clustering might be restricted which causes reduced cell proliferation.

Another possible facing problem of current nasal implant is implant infection. The implant related infection is one of the main causes of implant failures, which often require implant removal [19,20]. It is known that as long as the implant damages or invades epithelial or mucosa barriers, or serves as reservoirs for microorganisms, they are predisposed to infection. However, implant related infections are often difficult to treat. The main reason is the biofilm formation, an aggregate of microorganism adhering on a surface with resistance to host

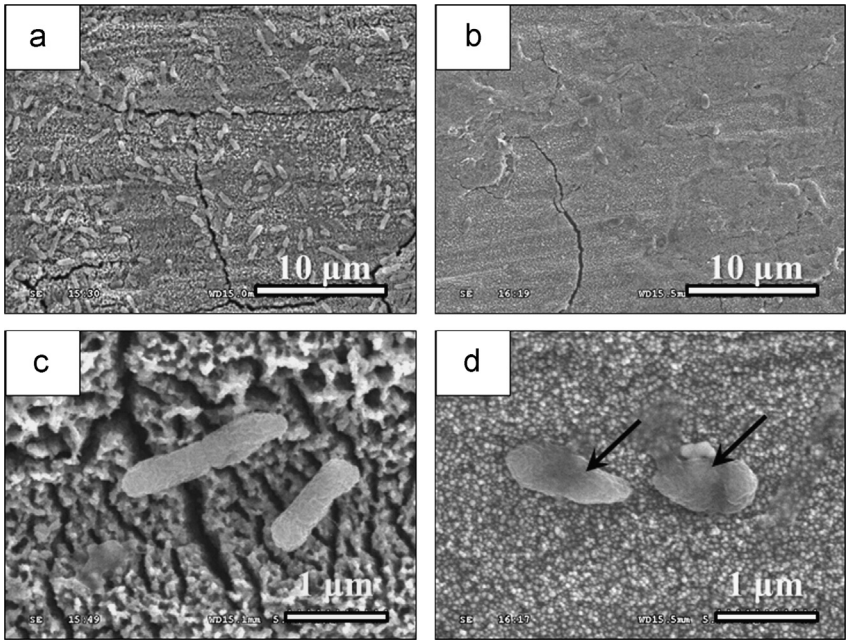

Fig. 5. SEM images of *Pseudomonus aeruginosa* grown on as-grown or Ag-coated TiO_2 nanotubes with the diameter of 25 nm. Numerous bacteria colonize on the as-grown 25-nm-diameter nanotubes (a), while only a few bacteria can be seen on the Ag-coated nanotubes (b). Some of the bacteria on the Ag-coated TiO_2 nanotubes presented with deformity as indicated by the arrows in (d), which is not found in those on as-grown samples (c).

defense system and antibiotic treatment. Several factors are related to biofilm formation on the implant surface: chemical composition of the material, surface roughness, surface configuration, and surface hydrophobicity [20]. Surface characteristics, such as irregular and porous surface, and hydrophobic materials, predispose implants to bacteria colonization [20]. Since biofilm formation is dependent upon a surface, surface modification to make implant hostile to microorganisms, is a potential strategy to be considered. Ag, one of the oldest known antimicrobials, is now used widely to combat microorganisms in wounds and burns. They show a broad antibacterial effect against all bacteria and without problems of developing resistance [21,22]. The positively charged ionic form is highly toxic for microorganisms but has relatively low toxicity for human tissue cells. Therefore, Ag coated implant provides an antibacterial strategy for biomaterials.

In our study, we decorated TiO_2 nanotubes with the silver particles on its surface by the e-gun vacuum evaporation system. The results show that the Ag-coated TiO_2 nanotubes revealed antibacterial effect against *P. aeruginosa*. The antibacterial effect of Ag may be explained by several mechanisms. It can react with negatively charged side groups of the proteins on the bacterial membrane, resulting in membrane destruction [23–25]; it can combine with DNA to inactivate its synthesis and translation [26]; it can also interrupt protein folding and function, electron transport, and even cell wall synthesis [21,22]. Moreover, it can produce reactive oxygen species (ROS) which causes significant cell damage [27]. This is why Ag possesses the advantages of broad spectrum antibacterial activity and extremely rare bacterial resistance. It is known that metallic Ag has no antimicrobial effect unless it undergoes oxidation to release ionic form. The limitation of ionic Ag is that they are only active for a short period of time (a few days). On the contrary, metallic Ag nanoparticles persist in delivering antimicrobial Ag for as long as 100-200 days. Furthermore, Ag nanoparticles possess a greater ratio of surface area to volume compare to same weight of a solid Ag sphere, thus provide a greater area available for oxidation necessary for continuously releasing Ag ions [21]. The three-dimensional exposure of Ag nanoparticles on the Ti sheet additionally provides a large surface area for contacting with bacteria, which enhances its antibacterial effect. Therefore, our designed Ag-coated TiO_2 nanotubes could provide a sustained Ag release, which may kill surrounding bacteria after implantation to prevent possible post-operation infection during initial stage of wound healing.

Although there are similarly designed Ag-coated TiO_2 implants in other research groups [19,28–30], differences still exist. In Flores's study, they developed a simple method to modify Ti/TiO_2 with Ag nanoparticles which exhibits a good resistance to colonization by *P. aeruginosa* [19]. Chang et al. found the amount of Ag in the TiO_2/Ag compound coating on Ti-based plates has an effect on the inhibition of bacterial growth and there is no difference of cell proliferation between TiO_2/Ag-coated samples and uncoated Ti [28]. In Liao's study, they demonstrated that Ti plates deposited by nanosilver showed both good antibacterial properties and uncompromised cytocompatibility [29,30]. Above studies, they coated Ag simply on Ti sheets without nanostructures, while we coated Ag on different sizes of TiO_2 nanotubes. Our Ag-coated TiO_2 nanotubes provide good biocompatibility, and also serve as a large reservoir for Ag which can result in long-term antibacterial effect. Uhm et al. applied silver nanoparticles to TiO_2 nanotube with e-beam evaporation which showed antibacterial activity, but small diameter ones showed mild cytotoxicity while large-diameter TiO_2 nanotubes had favorable osteogenic properties [31]. The result of Uhm's study was not the same as ours. Another two studies developed around 100 nm Ag-coated TiO_2 nanotubes, and both products provided antibacterial properties without compromising cytocompatibility [32,33]. Our study developed 3 different diameter sizes of Ag-coated TiO_2 nanotubes and found the smallest one, 25 nm, possesses both good cytocompatibility and effective antibacterial activity.

In summary, our results showed that 25-nm-diameter Ag-coated TiO_2 nanotubes possess both good cytocompatibility on cultured HNEpCs and antibacterial activity against *P. aeruginosa*. Further animal models merit investigation to see if applying this method clinically is suitable.

5. Conclusion

The study revealed that 25-nm-diameter Ag-coated TiO_2 nanotubes are biocompatible with HNEpCs and are antibacterial against *P. aeruginosa*, compared to 50- and 100-nm-diameter nanotubes. Therefore, such small-nanometer Ag-coated TiO_2 nanotubes might be a potential novel nasal implant in the future.

Acknowledgments

The research was supported by the Veterans General Hospitals University System of Taiwan Joint Research Program under Contract nos. VGHUST101-G4-3-1 and VGHUST101-G4-3-2, and by the National Science Council of Taiwan under Contract no. NSC-100-2221-E-008-016-MY3. The authors also thank the Center for Nano Science and Technology at National Central University and Clinical Research Core Laboratory at Taipei Veterans General Hospital for their support.

References

[1] G.R. Holt, Grafts and implants in facial, head, and neck surgery, in: B.J. Bailey, J.T. Johnson, S.D. Newlands (Eds.), Head & Neck Surgery—Otolaryngology, Lippincott Williams & Wilkins, Philadelphia, PA, 2006, pp. 2345–2356.

[2] A.W. Tan, B. Pingguan-Murphy, R. Ahmad, S.A. Akbar, Review of titania nanotubes: Fabrication and cellular response, Ceramics International 39 (2012) 4899–4906.

[3] M. Friedman, R. Vidyasagar, Surgical management of septal deformity, turbinate hypertrophy, nasal valve collapse, and choanal atresia, in: B. J. Bailey, J.T. Johnson, S.D. Newlands (Eds.), Head & Neck Surgery—Otolaryngology, Lippincott Williams & Wilkins, Philadelphia, PA, 2006, pp. 320–335.

[4] J.B. Heller, J.S. Gabbay, A. Trussler, M.M. Heller, J.P. Bradley, Repair of large nasal septal perforations using facial artery musculomucosal flap, Annals of Plastic Surgery 55 (2005) 456–459.
[5] L. Persutti, M. Alicandri Ciufelli, D. Marchioni, D. Villari, A. Marchetti, F. Mattioli, Nasal septal perforation: our surgical technique, Otolaryngology-Head Neck Surgery 136 (3) (2007) 369–372.
[6] J.R. Coleman Jr., E.B. Strong, Management of nasal septal perforation, Current Opinion in Otolaryngology and Head and Neck Surgery 8 (2000) 58–62.
[7] D.N. Fairbanks, G.R. Fairbanks, Nasal septal perforation: prevention and management, Annals of Plastic Surgery 5 (1980) 452–459.
[8] M. Friedman, H. Ibrahim, V. Ramakrishnan, Inferior turbinate flap for repair of nasal septal perforation, Laryngoscope 113 (2003) 1425–1428.
[9] A. Daneshi, S. Mohammadi, M. Javadi, F. Hassannia, Repair of large nasal septal perforation with titanium membrane: report of 10 cases, American Journal of Otolaryngology 31 (2010) 387–389.
[10] C. Deng, R. Li, J. Yang, Q. Huang, L. Xu, Repairing large perforation of nasal septum with titanium membrane and local pedicled mucoperiosteum flap, Lin Chuang Er Bi Yan Hou Ke Za Zhi 20 (2006) 358–359.
[11] E.L. Henry, R.D. Hart, S. Mark Taylor, J.R. Trites, J. Harris, D.A. O'Connell, H. Seikaly, Total nasal reconstruction: use of a radial forearm free flap, titanium mesh, and a paramedian forehead flap, Journal of Otolaryngology-Head and Neck Surgery 39 (6) (2010) 697–702.
[12] H.F. Marao, J.L. Gulinelli, C.C. Pereira, A.C. Carvalho, P.E. Faria, F.O. Magro, Use of titanium mesh for reconstruction of extensive defects in fronto-orbito-ethmoidal fracture, The Journal of Craniofacial Surgery 21 (2010) 748–750.
[13] M.A. Rodriguez-Prieto, A. Perez-Bustillo, T. Alonso-Alonso, P. Sanchez-Sambucety, Partial nasal reconstruction with titanium mesh: report of five cases, British Journal of Dermatology 161 (2009) 683–687.
[14] M.A. Rodriguez-Prieto, T. Alonso-Alonso, P. Sanchez-Sambucety, Nasal reconstruction with titanium mesh, Dermatologic Surgery 35 (2009) 282–286.
[15] U. Raghavan, N.S. Jones, The complications of giant titanium implants in nasal reconstruction, Journal of Plastic Reconstructive and Aesthetic Surgery 59 (2006) 74–79.
[16] F. Esposito, J.R. Dusick, N. Fatemi, D.F. Kelly, Graded repair of cranial base defects and cerebrospinal fluid leaks in transsphenoidal surgery, Neurosurgery 60 (4 Suppl 2) (2007) 295–304.
[17] M.Y. Lan, C.P. Liu, H.H. Huang, J.K. Chang, S.W. Lee, Diameter-sensitive biocompatibility of anodic TiO_2 nanotubes treated with supercritical CO_2 fluid, Nanoscale Research Letter 8 (2013) 150.
[18] J. Park, S. Bauer, K. von der Mark, P. Schmuki, Nanosize and vitality: TiO_2 nanotube diameter directs cell fate, Nano Letters 7 (2007) 1686–1691.
[19] C.Y. Flores, C. Diaz, A. Rubert, G.A. Benitez, M.S. Moreno, M.A. Fernández Lorenzo de Mele, R.C. Salvarezza, P.L. Schilardi, C. Vericat, Spontaneous adsorption of silver nanoparticles on Ti/TiO_2 surfaces. Antibacterial effect on Pseudomonas aeruginosa, Journal of Colloid and Interface Science 350 (2) (2010) 402–428.
20 K.D.O. Boahene, Synthetic implants, in: I.D. Papel (Ed.), Facial Plastic and Reconstructive Surgery, Thieme, New York, 2009, pp. 67–75.
[21] B. Gibbins, L. Warne, The role of antimicrobial silver nanotechnology, Medical Device and Diagnostic Industry 8 (2005) 2–5.
[22] K. Chaloupka, Y. Malam, A.M. Seifalian, Nanosilver as a new generation of nanoproduct in biomedical applications, Trends in Biotechnology 28 (11) (2010) 580–588.
[23] D.W. Hatchett, H.S. White, Electrochemistry of sulfur adlayers on the low-index daces of silver, The Journal of Physical Chemistry 100 (1996) 9854–9859.
[24] T. Vitanov, A. Popov, Adsorption of SO_4^{2-} on growth steps of (111) and (100) faces of silver single crystals, Journal of Electroanalytical Chemistry 159 (1983) 437–441.
[25] I. Sondi, B. Salopek-Sondi, Silver nanoparticles as antimicrobial agent: a case study on *E. coli* as a model for Gram-negative bacteria, Journal of Colloid and Interface Science 275 (2004) 177–182.
[26] Q.L. Feng, J. Wu, G.Q. Chen, F.Z. Cui, T.N. Kim, J.O. Kim, A mechanistic study of the antibacterial effect of silver ions on *Escherichia coli* and *Staphylococcus aureus*, Journal of Biomedical Materials Research 52 (4) (2000) 662–668.
[27] H.J. Park, J.Y. Kim, J. Kim, J.H. Lee, J.S. Hahn, M.B. Gu, J. Yoon, Silver-ion-mediated reactive oxygen species generation affecting bactericidal activity, Water Research 43 (4) (2009) 1027–1032.
[28] Y.Y. Chang, C.H. Lai, J.T. Hsu, C.H. Tang, W.C. Liao, H.L. Huang, Antibacterial properties and human gingival fibroblast cell compatibility of TiO_2/Ag compound coatings and ZnO films on titanium-based material, Clinical Oral Investigations 16 (1) (2012) 95–100.
[29] L. Juan, Z. Zhimin, M. Anchun, L. Lei, Z. Jingchao, Deposition of silver nanoparticles on titanium surface for antibacterial effect, International Journal of Nanomedicine 5 (2010) 261–567.
[30] J. Liao, M. Anchun, Z. Zhu, Y. Quan, Antibacterial titanium plate deposited by silver nanoparticles exhibits cellcompatibility, International Journal of Nanomedicine 5 (2010) 337–342.
[31] S.H. Uhm, D.H. Song, J.S. Kwon, S.B. Lee, J.G. Han, K.M. Kim, K.N. Kim, E-beam fabrication of antibacterial silver nanoparticles on diameter-controlled TiO_2 nanotubes for bio-implants, Surface and Coatings Technology 228 (2013) S360–S366.
[32] K. Das, S. Bose, A. Bandyopadhyay, B. Karandikar, B.L. Gibbins, Surface coatings for improvement of bone cell materials and antimicrobial activities of Ti implants, Journal of Biomedical Materials Research Part B: Applied Biomaterials 87 (2) (2008) 455–460.
[33] L. Zhao, H. Wang, K. Huo, L. Cui, W. Zhang, H. Ni, Y. Zhang, Z. Wu, P.K. Chu, Antibacterial nano-structured titania coating incorporated with silver nanoparticles, Biomaterials 32 (2011) 5706–5716.